6896 *Biochemistry* **2010,** *49,* 6896–6902
DOI: 10.1021/bi100739r

BIOCHEMISTRY
including biophysical chemistry & molecular biology
Article

Modulation of the Oligomerization of Myelin Proteolipid Protein by Transmembrane Helix Interaction Motifs[†]

Derek P. Ng and Charles M. Deber*

Division of Molecular Structure and Function, Research Institute, Hospital for Sick Children, Toronto, Ontario, Canada M5G 1X8, and Department of Biochemistry, University of Toronto, Toronto, Ontario, Canada M5S 1A8

Received May 10, 2010; Revised Manuscript Received July 13, 2010

ABSTRACT: Proteolipid protein (PLP) is a highly hydrophobic 276-residue integral membrane protein that constitutes more than 50% of the total protein in central nervous system myelin. Previous studies have shown that this protein exists in myelin as an oligomer rather than as a monomer, and mutations in PLP that lead to neurological disorders such as Pelizaeus-Merzbacher disease and spastic paraplegia type 2 have been reported to affect its normal oligomerization. Here we employ peptide-based and in vivo approaches to examine the role of the TM domain in the formation of PLP quaternary structure through homo-oligomeric helix−helix interactions. Focusing on the TM4 α-helix (sequence ^{239}FIAAFVGAAATLVSLLTFMIAATY^{262}), the site of several disease-causing point mutations that involve putative small residue helix−helix interaction motifs in the TM4 sequence, we used SDS−PAGE, fluorescence resonance energy transfer, size-exclusion chromatography, and TOXCAT assays in an *Escherichia coli* membrane to show that the PLP TM4 helix readily assembles into varying oligomeric states. In addition, through targeted studies of the PLP TM4 α-helix with point mutations that selectively eliminate these small residue motifs via substitution of Gly, Ala, or Ser residues with Ile residues, we describe a potential mechanism through which disease-causing point mutations can lead to aberrant PLP assembly. The overall results suggest that TM segments in misfolded PLP monomers that expose and/or create surface-exposed helix−helix interaction sites that are normally masked may have consequences for disease.

Membrane proteins constitute ~20−30% of all proteins in sequenced genomes (*1*) and have functions ranging from signal transduction to the movement of ions and other solutes across the cell membrane. Many of these proteins assemble into oligomers and do so in specific patterns that minimize uncontrolled proliferation (*2*). Oligomerization is often required for function and, in some membrane proteins, for successful exit from the endoplasmic reticulum (*3*).

Studies of oligomer formation by single-spanning membrane proteins have revealed that transmembrane (TM)[1] α-helices often play a critical role in assembly by providing sequence-specific helix−helix interaction motifs that stabilize the higher-order structures (*4*). These motifs, including GxxxG (so-called "small-xxx-small" motifs), heptad repeats, and polar residues, stabilize helix−helix contacts by maximizing van der Waals interactions and/or allowing the formation of side chain−side chain hydrogen bonds at the helix-packing interfaces (*5*). Several multispan membrane proteins are reported to utilize similar helix−helix interactions for oligomerization; for example, the Leu heptad repeat in TM2 of Na^+Cl^--dependent neurotransmitter transporter GAT-1, the PxxxM motif in TM5 of G-protein-coupled receptor A2AR, and the small-residue heptad repeat in TM4 of the small multidrug resistance protein Hsmr are required for oligomer stability (*6*−*9*).

Proteolipid protein (PLP) is a multispan 276-residue integral membrane protein that is anchored to the lipid bilayer via four TM α-helices and several fatty acids that are conjugated to cysteines in the intracellular region of the protein (*10*). PLP is thought to maintain and stabilize the lamellar structure of central nervous system (CNS) myelin mainly through adhesion of the extracellular surfaces of the myelin membranes, but other functions, including ion channel and signaling, have been proposed (*11*−*13*). This protein has been shown to be capable of oligomerization, as determined by biophysical techniques, including spin-label electron spin resonance (hexamer in DMPC), sedimentation equilibrium (hexamer in deoxycholate and Triton X-100), co-immunoprecipitation, and native/SDS−PAGE (dimer/trimer in cell lysates and myelin) (*14*−*18*). Although the general topology of this membrane protein has been extensively studied (*10*, *19*), the molecular structure of the TM domain of the PLP monomer and its possible role in PLP oligomer formation have not been examined. In this work, we utilize peptide-based and in vivo approaches to examine the potential TM-mediated mechanism of

[†]Supported, in part, by a grant to C.M.D. from the Canadian Institutes of Health Research (CIHR FRN5810). D.P.N. holds a Frederick Banting and Charles Best Canada Graduate Scholarship (CGS) Doctoral Award from CIHR.

*To whom correspondence should be addressed: Division of Molecular Structure and Function, Research Institute, Hospital for Sick Children, 555 University Ave., Toronto, Ontario, Canada M5G 1X8. Telephone: (416) 813-5924. Fax: (416) 813-5005. E-mail: deber@sickkids.ca.

[1]Abbreviations: PLP, proteolipid protein; TM, transmembrane; SDS, sodium dodecyl sulfate; FRET, fluorescence resonance energy transfer; SEC, size-exclusion chromatography; CNS, central nervous system; DMPC, dimyristoylphosphatidylcholine; DMF, dimethylformamide; DIEA, *N*,*N*-diisopropylethylamine; TFA, trifluoroacetic acid; TIPS, triisopropylsilane; RP-HPLC, reverse phase high-performance liquid chromatography; MW, molecular weight; CD, circular dichroism; TFE, 2,2,2-trifluoroethanol; MW_{app}, apparent molecular weight; GPA, glycophorin A; CAT, chloramphenicol acetyltransferase; PMD, Pelizaeus-Merzbacher disease; SPG2, spastic paraplegia type 2; MBP, maltose binding protein.

 Published on Web 07/13/2010

PLP oligomer assembly. Through systematic substitutions of the putative helix−helix interaction motifs in the PLP TM4 α-helix, we assess the structural impact of disease-causing point mutations that target the residues in these motifs and suggest a mechanism by which this α-helix may modulate PLP quaternary structure.

EXPERIMENTAL PROCEDURES

TM Helix Prediction. The amino acid sequence of bovine PLP was obtained from Swiss-Prot (accession number P04116) and submitted to the TM predicting program web servers described previously (*20*). Default values were used in all programs. The amino acid numbering for PLP begins after the initiator methionine.

Peptide Synthesis and Labeling. Peptides were synthesized using Fmoc chemistry on a PS3 peptide synthesizer (Protein Technologies, Inc.) using the protocol from the manufacturer. A 4-fold excess of amino acids on a 0.1 mmol scale was used with the HATU/DIEA activator pair. An amidated C-terminus was produced using a low-load (0.18−0.22 mmol/g) PAL-PEG-PS resin. For FRET experiments, peptides were labeled with dansyl chloride and dabsyl chloride (Molecular Probes) as follows: 100 mg of resin containing covalently attached peptide (such that the only reactive site is the amino group of the N-terminal residue) was incubated overnight in 10 mg of label with 1 mL of DMF and 50 μL of DIEA (room temperature, in the dark, under nitrogen, with stirring). This reaction was repeated to enhance labeling. Peptides were cleaved from the resin using a cocktail consisting of 88% TFA, 5% phenol, 5% ultrapure water, and 2% TIPS. The cleaved peptides were subsequently precipitated and washed with ice-cold diethyl ether, air-dried, and redissolved in ultrapure water. For purification, peptides were loaded onto a C4 preparative RP-HPLC column (Phenomenex), and the major peaks from a water/2-propanol gradient were collected. Peptide MWs were confirmed by mass spectrometry. Samples were lyophilized, redissolved in ultrapure water, and stored at −20 °C. Peptide concentrations were determined using the Micro BCA assay (Pierce) and quantitative amino acid analysis.

Circular Dichroism (CD) Spectroscopy. Peptides were diluted to a final concentration of 15 μM in aqueous buffer [10 mM Tris-HCl and 10 mM NaCl (pH 7.2)], aqueous buffer with 20 mM SDS, or 96% (v/v) 2,2,2-trifluoroethanol (TFE). Samples in aqueous buffer or aqueous buffer with SDS were allowed to equilibrate overnight at RT prior to being read in a Jasco J-720 circular dichroism spectropolarimeter. The TFE samples were read within 30 min of preparation. The path length of the cuvette was 0.1 cm. Spectral scans were performed from 250 to 190 nm with a step resolution of 0.1 nm, a bandwidth of 2 nm, and a speed of 50 nm/min. Three scans were acquired and averaged per sample, and all experiments were performed in triplicate. Background spectra without peptide were subtracted.

SDS−PAGE. Gel boxes, gels (18% Tris-glycine and 12% NuPAGE), and buffers were purchased from Novex Corp. PAGE was conducted according to the manufacturer's instructions. Peptides were resuspended in sample buffer and incubated at room temperature for >15 min prior to being loaded on the gel. Peptides were visualized with either silver stain using the SilverXpress Silver Staining Kit (Invitrogen) following the manufacturer's instructions or Coomassie Brilliant Blue R-250 stain. Apparent molecular weights (MW_{app}) were estimated from the migration of Novex Sharp unstained protein standards (Invitrogen) and were averaged from at least three independent gel runs. Decreases in the rate of migration from the lysine tags were taken into account when calculating the MW_{app} (*21*). ImageJ (National Institutes of Health) was used to analyze the gels.

Fluorescence Resonance Energy Transfer (FRET) Titrations. FRET experiments were conducted using dansyl-labeled peptides (donor) in the presence of increasing mole fractions of dabsyl-labeled peptides (acceptor). The dansyl-labeled peptide concentration was maintained at either 1 or 2 μM as the mole fraction of dabsyl-labeled peptide was increased for a total peptide concentration of 5 or 10 μM, respectively. The addition of unlabeled peptide was used to keep the total peptide concentration constant. Peptides were mixed prior to the addition of the buffer and SDS. Samples were then allowed to equilibrate at room temperature overnight before being read in a 0.1 cm cuvette by a Photon Technology International C-60 spectrofluorimeter. Experiments were conducted in 20 mM SDS, 10 mM Tris-HCl, and 10 mM NaCl (pH 7.2). The excitation wavelength was set to 341 nm with a 4 nm bandpass, and emission spectra were recorded from 450 to 600 nm with a 4 nm bandpass at a scanning speed of 1 nm/0.3 s and an average of three scans. All samples were analyzed in triplicate. Spectra were integrated between 450 and 600 nm using FELIX provided by the manufacturer. Integrated total fluorescence intensities at each point in the titration (F) were normalized by the initial integrated total fluorescence intensity in the absence of acceptor peptide (F_0). The mole fraction acceptor (P_A) was calculated according to the relation

$$P_A = \frac{[\text{acceptor peptide}]}{[\text{total peptide}]}$$

Data were fit as described previously (*22*) using Kaleidagraph.

Size-Exclusion Chromatography (SEC). SEC-HPLC was performed on a 7.8 mm × 300 mm BioSep SEC-S2000 column (Phenomenex) equilibrated and run at a rate of 0.5 mL/min with 0.3% high-purity SDS (BioUltra, Fluka) and 50 mM sodium phosphate (pH 7). The purified TM4 peptide was dissolved in 300 μL of mobile phase buffer (at various peptide amounts), allowed to equilibrate at room temperature overnight, and microcentrifuged at maximum speed for 15 min at room temperature before injection. The elution profile was measured using an absorbance at 215 nm. The void volume was determined using blue dextran 2000 (GE Healthcare).

TOXCAT Chimera Construction. Expression vectors pccKan and pccGpA-WT, along with *Escherichia coli* strain NT326 (*malE*$^-$), were kindly provided by D. Engelman (Yale University, New Haven, CT) (*23*). The ToxR-stop construct was kindly provided by J. Mogridge (University of Toronto) (*24*). The TOXCAT constructs contain an N-terminal ToxR DNA binding domain, a transmembrane domain, and a periplasmic maltose binding protein (MBP) domain. Oligonucleotides encoding the amino acid sequence of PLP TM4 were restriction digested with *Nhe*I and *Bam*HI and ligated into the *Nhe*I and *Bam*HI sites of the restriction-digested pccKAN plasmid. Individual mutants of TM4 were produced via mutation of the WT construct using the QuikChange site-directed mutagenesis kit (Stratagene, La Jolla, CA). The sequences of all constructs were confirmed using DNA sequencing and subsequently transformed into *E. coli* NT 326 (*malE*$^-$) cells.

Chloramphenicol Acetyltransferase (CAT) Enzyme-Linked Immunosorbent Assay. NT326 cells transformed with the TOXCAT chimeras were grown at 37 °C, harvested into 1 mL

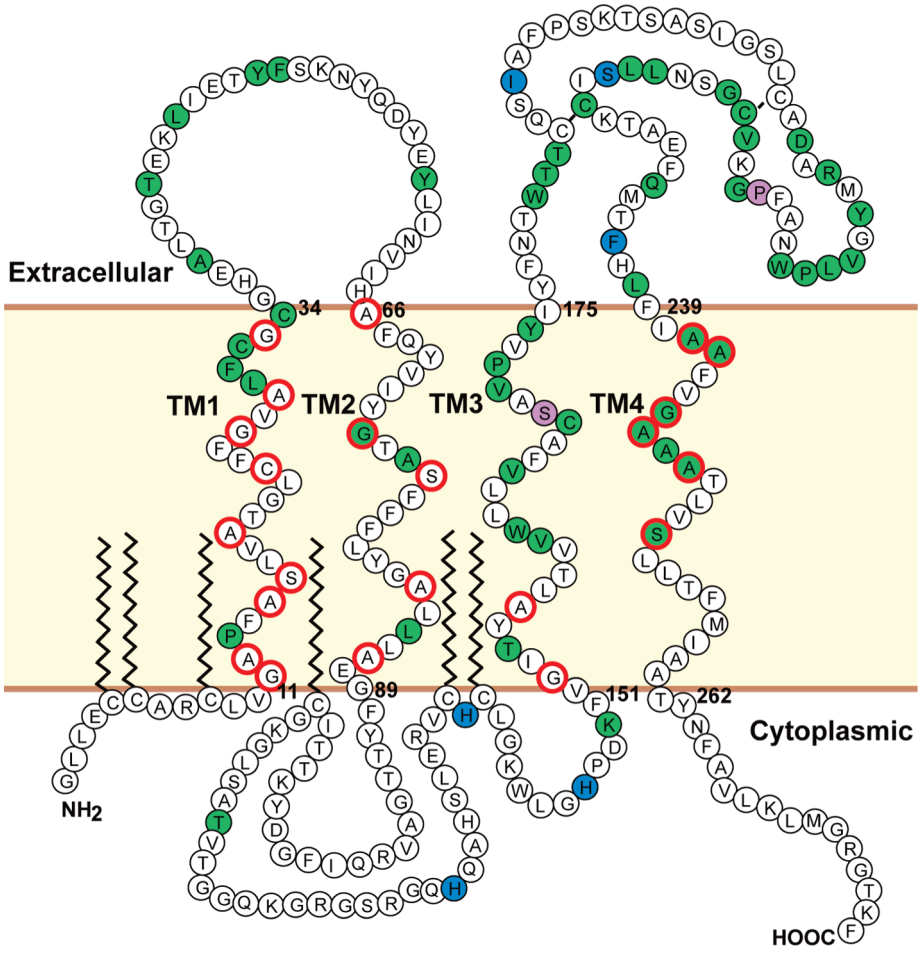

FIGURE 1: Topology map of known proteolipid protein (PLP) disease-causing point mutations and putative TM domain oligomerization motifs. Sites of known disease-causing point mutations in PLP were obtained from the Human Gene Mutation Database (*35*) and plotted onto a topology map of the protein primary structure. Point mutations causing Pelizaeus-Merzbacher disease (PMD), spastic paraplegia type 2 (SPG-2), or both are colored green, blue, and purple, respectively. Residues highlighted by red circles constitute putative helix−helix interaction motifs (GAS_{left} and GAS_{right}). The lines in the extracellular domain connecting the cysteines denote disulfide bridges; the extended zigzag lines in the cytoplasmic domain represent thioester-linked fatty acids.

fractions at an A_{600} of 0.6, pelleted, and stored at −80 °C. Cell lysates were prepared from cell pellets as previously described (*25*) and assayed for CAT concentration using the CAT enzyme-linked immunosorbent assay kit (Roche Applied Science). A standard curve was generated with CAT provided by the manufacturer. Cells expressing wild-type GpA and the ToxR truncation mutant (ToxR-stop) were included in each CAT assay as positive and negative controls, respectively. CAT measurements were performed in quadruplicate and were normalized for the relative expression level of each construct using Western blotting and densitometry as described previously (*25*). One-way Anova and Dunnett multiple comparison tests were used to determine statistically significant differences. The *MalE* complementation test was performed on all constructs as previously described (*25*) to ensure proper membrane insertion of the chimera protein.

RESULTS

Design of a Peptide for Modeling the PLP TM4 α-Helix. Because more than 40% of the known point mutations that cause PMD and SPG2 are located in the PLP TM domain, we focused on this domain as a potential mediator for oligomerization of the protein. In addition, the four TM α-helices contain multiple helix−helix interaction motifs (notably, GAS_{left} and GAS_{right}) (Figure 1) that have previously been shown in other single-pass and multipass membrane proteins to mediate oligomerization (*26*). The amino acid sequences most likely to comprise the four TM α-helices of human PLP were derived both from the consensus in previous literature (*27*) and from the output of several TM predicting programs (see Experimental Procedures) which aided in the delineation of membrane entry and exit boundaries. The sequences resulting from this output are designated [TM1] (PLP 11−34), [TM2] (66−91), [TM3] (151−177), and [TM4] (239−262). Consideration of the length and hydrophobic core of these peptide sequences indicates that they each meet the minimum threshold requirement for spontaneous insertion into a membrane environment (*28*, *29*).

Many of the disease-phenotypic mutations target the potential helix−helix interaction motifs in the PLP TM4 α-helix, indicating that this helix may be a potential interaction site for the PLP oligomer; importantly, all six of the TM4 residues involved in GAS_{right} and GAS_{left} motifs have been identified as disease-phenotypic mutation sites (Figures 1 and 2). We further noted that point mutations in the TM4 α-helix of the full-length protein (A242V and G245A, both of which constitute part of the putative helix−helix interaction motifs in this helix) have been shown to affect the oligomerization state of the protein, as well as retention in the ER (*14*, *30*). Accordingly, a peptide corresponding to the

```
          WT TM4:   239FIAAFVGAAATLVSLLTFMIAATY262
GAS_right GG4:        --A---G-----------------
                      ---A---A-----------------
                      ---------A---S----------
GAS_left heptad:      --A---G--A---S----------
```

FIGURE 2: PLP TM4 amino acid sequence and location of putative helix−helix interaction motifs. The amino acid sequence of PLP transmembrane segment 4 (TM4, residues 239−262) is shown. Residues in bold indicate locations of disease-causing point mutations. Each line below the TM4 sequence indicates the individual motif and the "small" residues that are typically important in these motifs. See Figure 1 for the TM4 sequence and Experimental Procedures for the estimation of boundary residues.

TM4 amino acid sequence was chemically synthesized; a total of eight Lys residues were added to the ends of the peptide (four Lys residues on each terminus) to increase solubility while preserving the native properties of the hydrophobic TM4 segment. Figure 3 shows the CD spectra of the resulting TM4 peptide in the absence and presence of SDS, as well as in 2,2,2-trifluoroethanol (TFE), both of which are often employed as membrane mimetics. As expected for a TM α-helix, the peptide adopts α-helical conformations in both SDS and TFE as indicated by the double minima at 208 and 222 nm. In aqueous buffer, this peptide has only minimal α-helical content.

PLP TM4 Can Self-Associate in SDS Micelles. To determine whether the wild-type (WT) TM4 α-helix is capable of mediating PLP oligomerization, the TM4 peptide was analyzed via SDS−PAGE. In soluble proteins, SDS tends to be denaturing, whereas in membrane proteins, it can drive secondary, tertiary, and/or quaternary structure formation (*7*); as such, this technique is often used to examine the oligomeric states of membrane proteins. Figure 4A shows the results of loading varying amounts of TM4 peptide on 18% Tris-glycine gels. The specific oligomeric states indicated by the band positions were estimated by normalization of the MW_{app} determined from the gel with the theoretical MW of the peptide. Quantitation of the darkest bands in each lane indicated that the estimated oligomeric size of TM4 shifted from 2.1 ± 0.05 to 3.9 ± 0.02 when the amount of peptide loaded was increased from 0.05 to 5 μg. The multiple bands or smears in each lane likely represent separate oligomeric species because the peptide migrates as a single band on NuPAGE gels (data not shown), a system that is not typically capable of resolving multiple oligomeric species (*31*).

To confirm that the change in migration of the TM4 peptide in SDS−PAGE is due to a change in oligomeric state, we employed FRET titration experiments. Here, localization of dansyl- and dabsyl-labeled peptides within 40 Å results in energy transfer and a stoichiometry-dependent quenching of the donor (dansyl) by the acceptor (dabsyl) peptide (*22*). The titration data for the TM4 peptide in SDS at various total peptide concentrations are shown in Figure 4B. Consistent with SDS−PAGE experiments, the FRET titration profile of the peptide is a function of the peptide concentration; at 10 μM, the TM4 peptide shows a nonlinear dependence of the fluorescence on acceptor mole fraction with a fit resulting in a tetramer ($n = 4.1 \pm 0.4$; $R^2 = 0.99$), whereas at 5 μM, the fit indicates an approximately dimeric state ($n = 2.5 \pm 0.2$; $R^2 = 0.99$).

Further support for the titratable oligomeric behavior of TM4 comes from size-exclusion chromatography. SEC chromatograms for TM4 injected onto the column at various peptide amounts are shown in Figure 5. It may be noted that the peptide

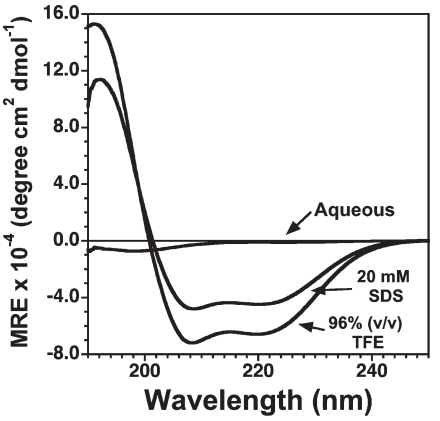

FIGURE 3: PLP TM4 secondary structure determined by circular dichroism spectroscopy. CD spectra of the TM4 peptide (15 μM) in aqueous buffer containing 10 mM Tris-HCl and 10 mM NaCl (pH 7.2), aqueous buffer with 20 mM SDS, or 96% (v/v) trifluoroethanol (TFE).

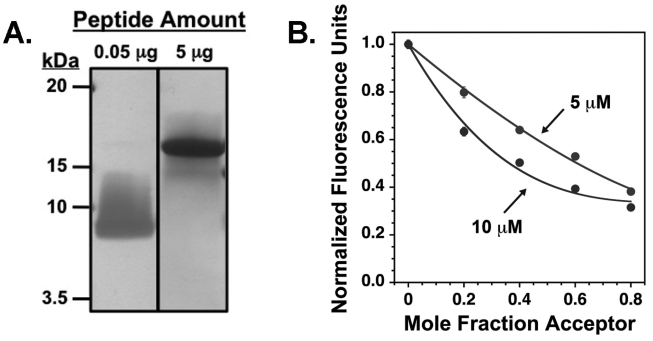

FIGURE 4: Oligomer formation of PLP TM4 in SDS. (A) TM4 peptide loaded onto 18% Tris-glycine gels at 0.05 μg (left) or 5 μg (right) of peptide for SDS−PAGE analysis. Bands were visualized using silver stain and Coomassie blue, respectively. (B) FRET experiments. Dansyl-labeled TM4 peptides (donor) were titrated with an increasing mole fraction of dabsyl-labeled peptides (acceptor) in 20 mM SDS, 10 mM Tris-HCl, and 10 mM NaCl (pH 7.2). The total peptide concentration was kept constant at either 5 or 10 μM by the addition of unlabeled peptide. Dansyl-labeled donor peptides were excited at 341 nm, and emission was measured from 450 to 600 nm. Plots were generated and data fit as described in Experimental Procedures; the lines shown represent the best fit to each data set. Error bars correspond to the standard deviation of at least three experiments.

amounts loaded in the SEC experiments (0.0143, 0.287, and 2.87 nmol) span a range similar to that used in SDS−PAGE experiments (Figure 4A), where 0.05 and 5.0 μg correspond to 0.014 and 1.40 nmol, respectively. Other than a fraction of the peptide that aggregates on the column [indicated by the small peak at the void volume (Figure 5, bottom)], the multiple peaks seen in the chromatograms at each concentration likely correspond to various oligomeric states of the purified peptide as observed via SDS−PAGE. One likely distribution of states would correspond to largely dimer for the TM4 helix at 0.014 nmol (Figure 4A, left; Figure 5, top, 27 min), along with two potential configurations of a TM4 tetramer between 1.40 nmol (PAGE) and 0.287−2.87 nmol (SEC) [i.e., parallel and antiparallel (Figure 4A, right; Figure 5, bottom and middle, 18 and 21 min)]. These results are also in broad agreement with the FRET experiments (Figure 4B).

PLP TM4 Can Self-Associate in a Natural Membrane Bilayer. To determine whether the helix−helix interactions mediating the TM4 oligomers in SDS are maintained when the

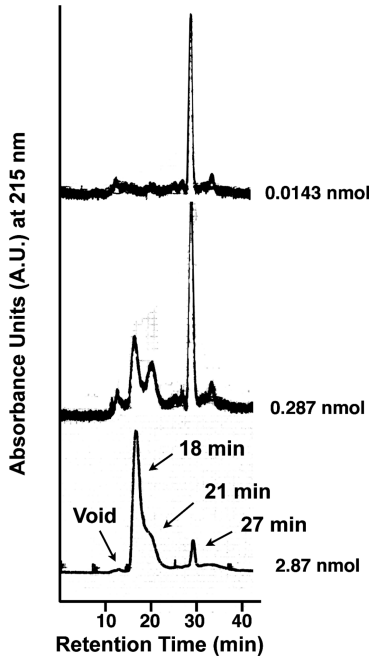

FIGURE 5: SDS SEC of PLP TM4. Size-exclusion chromatograms of the WT TM4 peptide at three different peptide loading amounts (0.0143, 0.287, and 2.87 nmol). Retention times of the major peaks are given.

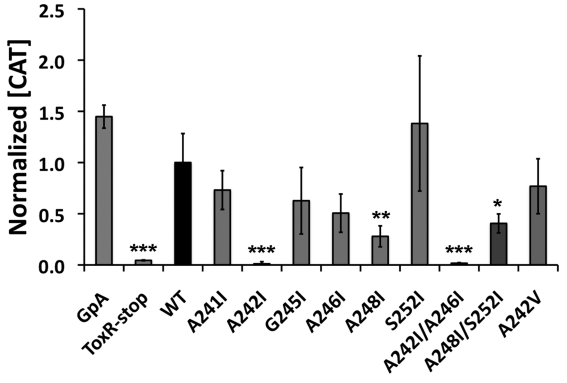

FIGURE 6: TOXCAT assays of PLP TM4 mutants. Constructs containing the PLP WT TM4 α-helix sequence and Ile point mutations studied in the TOXCAT assay. The bars indicate the amount of CAT expression normalized to WT TM4. GpA and a construct containing a stop codon in the ToxR gene (ToxR-stop) were used as positive and negative controls, respectively. Error bars correspond to the standard deviation of four experiments. *p* values were generated from a one-way Anova and Dunnett multiple-comparison tests (*$p < 0.05$; **$p < 0.01$; ***$p < 0.001$). See Experimental Procedures for a description of the TOXCAT assay.

helix is incorporated into a native-like lipid bilayer environment, we measured the relative helix−helix interaction strength in the in vivo TOXCAT assay (*23*). In this system, self-association of the TM α-helix drives the dimerization of the ToxR domain, resulting in the transcriptional activation of a reporter gene (CAT) that can be used as a measure of the extent of TM helix association. The levels of CAT expression for the PLP TM4 α-helix compared to the TM domain of glycophorin A (GpA), known to be a strong dimer (*23*), and to ToxR-stop, a truncation construct lacking the TM and MBP domains (*24*), are shown in Figure 6. We found that the TM4 construct results in a CAT expression level that is greater than that of the ToxR-stop construct ($p < 0.001$) and not statistically significantly different from that of the GpA construct, indicating that the TM4 α-helix is able to oligomerize in a bilayer membrane, albeit the TOXCAT assay does not specifically report or resolve greater-than-dimer states.

Identifying the Residues Mediating TM4 Oligomerization. As several putative GAS_{left} and GAS_{right} motifs are situated in the TM4 sequence (Figure 2), we examined the role of these residues in helix−helix interactions. Several sequence analogues of TM4 containing single- and double-site Ile point mutations at motif sites were prepared, with the expectation that the large volume of the Ile side chain could potentially disrupt any helix−helix packing normally mediated by WT small residues. The effects on the level of CAT expression of these point mutations compared to WT TM4 are shown in Figure 6. We found that two of these mutations showed statistically significant decreases versus WT, with A248I at a level of 0.28 ($p < 0.01$) and A242I reducing CAT expression to background levels ($p < 0.001$). When double-site Ile mutations were introduced, they generally did not cause disruption beyond that of the single-site point mutations; i.e., the A242I/A246I CAT level is dominated by A242I itself, and the A248I/S252I level is dominated by the A248I level rather than the S252I level.

It is important to note that the signal from the TOXCAT assay may be complicated by additional factors such as the length of the TM segment as this might affect the orientation of the soluble ToxR DNA-binding domain relative to the attached TM domain (*32*). For our TM4 mutation analysis, we have kept all of the constructs at similar TM lengths to minimize this effect.

Effect of a Disease-Causing Point Mutation on TM4 Oligomerization. Several disease-causing point mutations have been implicated in premature oligomerization of PLP and retention in the ER (*14*). Interestingly, the mutation leading to the most stable and rapidly formed PLP oligomer is the A242V (or *msd*) mutant. This well-studied mutation is known to cause the severe or connatal form of PMD in both humans and mice (*33*). On the basis of our experiments, A242I was noted as the mutant that totally abrogates helix−helix interactions in the TOXCAT assay (Figure 6). However, when we examined the effect of the corresponding A242V point mutation on the self-association of TM4, we found the level of CAT expression relative to the WT level was unchanged.

DISCUSSION

Membrane-embedded regions of proteins can mediate the formation of quaternary structure through sequence-specific interactions between the TM α-helices of the protein monomers (for a review, see ref *26*). The presence of a plethora of these putative helix−helix interaction motifs in the TM domain of PLP suggests that this membrane protein might also be utilizing, at least in part, a TM-mediated mechanism in its self-assembly (Figure 1). Here we employed a peptide approach to examine the potential for TM α-helix self-association in the TM domain of this protein. The use of peptides as models for the PLP TM α-helices circumvents the significant challenges involved in full-length PLP overexpression and purification (*34*) and has proven to be a valuable diagnostic of helix−helix interactions that mediate membrane protein oligomer formation (*5*).

The PLP TM4 helix is the site of a variety of disease-causing mutations [A241P, A242V, A242E, G245A, G245E, A246T, A247E, A248P, and S252F (*35*)], leading to the striking observation that mutations at small residue (G, A, and S) positions are pervasive. The indispensable importance of such small side chain residues in helix−helix dimerization and packing has been widely

observed in various systems, including the well-studied glycophorin A where, for example, mutations of G83 to larger residues abrogate dimerization (*36*). In this work, we demonstrate that a peptide containing the WT TM4 amino acid sequence is capable of self-association in SDS. In addition, we found that this TM peptide can access greater-than-dimer states; indeed, a single-TM peptide cannot physically form a discrete tetrameric state unless there is more than one "face" on the helix via which helix−helix interactions can occur (*2*).

The TOXCAT assay confirms the ability of the TM4 segment to at least dimerize when it is incorporated into the inner membrane of *E. coli*. It should be noted that a distinction between the TOXCAT and peptide/SDS−PAGE systems is that only parallel helix−helix interactions result in a CAT signal, while both parallel and antiparallel associations are equally accessible via SDS−PAGE. If the TM4 α-helix is involved in in vivo PLP self-association, it can do so only in a parallel manner due to the membrane topology of the full-length protein (*10*, *19*). As such, the results from the TOXCAT assay can be construed as being directly representative of the interactions that might occur in the native full-length protein, although one cannot directly determine from the TOXCAT assay per se whether TM4 is forming (parallel) higher-than-dimer states.

Disruption of Helix−Helix Association Motifs with Ile Mutations. The spacing among the small residues in the TM4 sequence (Figure 2) and their propensity for being targeted by disease-causing point mutations suggest that these amino acids may constitute helix−helix interaction motifs that mediate TM4 oligomer formation (*4*). In this context, we found that mutations of residues A242 and A248 to the large hydrophobic residue Ile significantly decrease the oligomer stability of the TM4 α-helix, indicating that these small residues likely mediate TM4 helix−helix interactions through optimal packing of the helix monomers. However, mutation of the remaining small residues (A241, G245, A246, and S252) to Ile had no effect on oligomer stability and suggests that the potential interaction motif(s) through which A242 and A248 mediate oligomer formation may not be as simple as a GAS_{right} or GAS_{left} motif, perhaps involving other residues not examined in this study.

When these results are plotted onto an idealized helix model and a helical wheel projection of TM4, A242 is located opposite from A248, suggesting that more than one helix−helix interaction face may be present (Figure 7). Interestingly, in the TOXCAT assay, the A242I mutation is completely disruptive whereas A248I is only partially disruptive. This may perhaps be explained by the coexistence of at least two populations of TM4 dimers and/or oligomers in the *E. coli* inner membrane: (i) a dimer formed by monomers interacting with their A242 faces and (ii) a dimer or oligomer formed by one monomer's A242 face interacting with another monomer's A248 face. Mutating A248 to Ile would then be partially disruptive, because only a subset of the dimers or oligomers generating TOXCAT signals would be affected compared to mutating A242 to Ile.

Role of Ile242 versus Val242 in PLP TM4. The extreme sensitivity of residue A242 in TM4 to Ile substitutions compared to A248 suggests that A242 plays a substantial role in the helix−helix interactions stabilizing the TM4 oligomer, yet a construct containing the disease-causing point mutation of this residue to Val behaved like WT TM4 in our TOXCAT analysis. This result is particularly intriguing, because *A242V* in the full-length protein causes premature or rapid oligomer formation and retention in the ER (*14*, *30*). It has been proposed that the

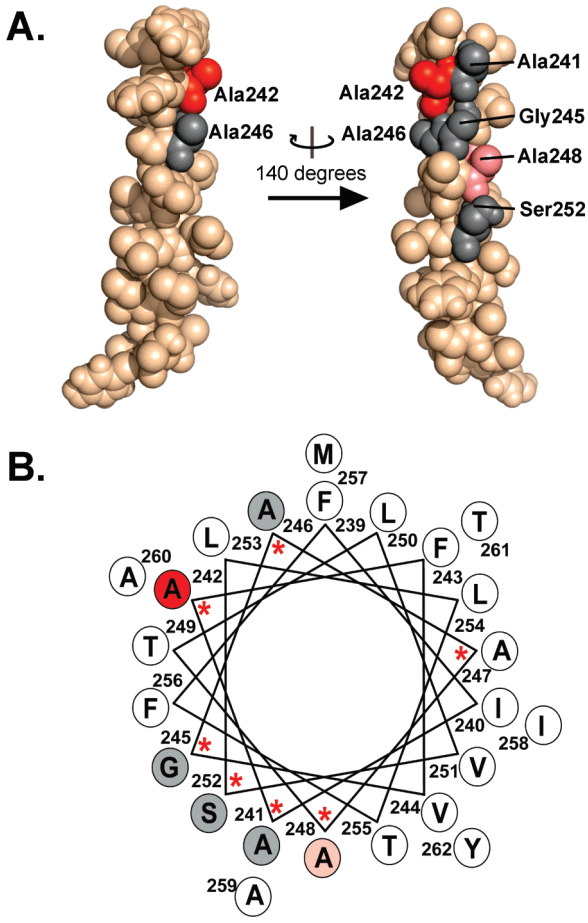

FIGURE 7: Space-filling models of the PLP TM4 helix. (A) Sequence of PLP TM4 modeled as an α-helix. Residues that were substituted with Ile in the TOXCAT assay (Figure 6) are highlighted. Those that were severely disruptive, moderately disruptive, and nondisruptive to TM4 self-association are colored red, pink, and gray, respectively. (B) Plot similar to panel A rendered as a helical wheel projection of TM4. Red stars denote the locations of disease-causing point mutations.

mutation to a β-branched residue may be enhancing TM helix−helix interactions by providing a conformationally restricted interface (*30*). What is clear is that the helix−helix packing at position 242 is critical: mutation of this residue to Val in the full-length PLP is perhaps sufficient to disrupt the native helix packing of the monomer such that the higher-affinity Val-containing "sticky" TM4 face is unmasked and drives non-native van der Waals interactions with TM4 of a second A242V PLP monomer, resulting in the observed premature oligomerization. Using this argument, the larger Ile side chain is ultimately too bulky to support a corresponding TM4−TM4 interaction face. It may be noted from the genetic code that single-base mutations are permissive for Val−Ala interchange, but not for Ile−Ala interchange; thus, A242I mutants would be extremely rare in nature (*37*). From a broader perspective, these findings highlight the divergent side chain−side chain interaction propensities of Ile and Val, despite the fact that these two residues are traditionally cocategorized as sharing many properties.

Non-Native TM Interactions and Disease. Preliminary TOXCAT data of sequences corresponding to PLP TM1, TM2, and TM3 α-helices indicate that, similar to TM4, they are able to self-associate (data not shown). As these three helices each contain at least one putative helix−helix interaction motif involving Gly, Ala, and/or Ser residues (Figure 1), their self-association is likely mediated by the availability of such interaction

motifs. In the intact PLP monomeric membrane domain, interhelical interactions (i.e., TM1−TM2, TM3−TM4, etc.) that promote its folding may consume several of these motifs such that once the PLP monomer has properly folded, it is likely that only the motifs remaining on the domain surface will be available to mediate protein oligomerization (*2*). The fact that several disease-causing point mutations cause premature oligomerization of PLP may be due to the mutations affecting the conformation of the monomer such that "sticky" helix faces that would normally be masked by the properly folded protein become surface-accessible, leading to aberrant assembly of the protein oligomer. The extent or amount of exposure of the TM4 (or other TM α-helix) faces and their mutual affinity may thus explain why various disease-causing point mutations in the PLP protein result in varying degrees of premature oligomerization (*14*). While one cannot estimate directly the extant concentration of PLP in vivo as it assembles in the plasma membrane, the fact that the protein will be concentrated into this microenvironment suggests that the sensitivity we observed of TM4 oligomeric states to concentration at micromolar levels may be relevant to the assembly process.

Although the overall results from this study do not pinpoint the structural consequences of all mutations in a unifying manner, the tendency of the individual TM segments to self-associate and the observation that Ile-based mutations tend to disrupt helix−helix packing motifs suggest that TM segments in misfolded PLP monomers that expose and/or create surface-exposed helix−helix interaction sites that are normally masked may have consequences for disease. The overall findings suggest that PLP, and likely other multispan membrane proteins, may exist on the "edge of aggregation" and help explain how mutation of a single amino acid may lead to aberrant protein assembly.

REFERENCES

1. Wallin, E., and von Heijne, G. (1998) Genome-wide analysis of integral membrane proteins from eubacterial, archaean, and eukaryotic organisms. *Protein Sci. 7*, 1029–1038.
2. Rath, A., and Deber, C. M. (2007) Membrane protein assembly patterns reflect selection for non-proliferative structures. *FEBS Lett. 581*, 1335–1341.
3. Sitte, H. H., Farhan, H., and Javitch, J. A. (2004) Sodium-dependent neurotransmitter transporters: Oligomerization as a determinant of transporter function and trafficking. *Mol. Interventions 4*, 38–47.
4. Mackenzie, K. R. (2006) Folding and stability of α-helical integral membrane proteins. *Chem. Rev. 106*, 1931–1977.
5. Rath, A., Johnson, R. M., and Deber, C. M. (2007) Peptides as transmembrane segments: Decrypting the determinants for helix-helix interactions in membrane proteins. *Biopolymers 88*, 217–232.
6. Poulsen, B. E., Rath, A., and Deber, C. M. (2009) The assembly motif of a bacterial small multidrug resistance protein. *J. Biol. Chem. 284*, 9870–9875.
7. Rath, A., Melnyk, R. A., and Deber, C. M. (2006) Evidence for assembly of small multidrug resistance proteins by a "two-faced" transmembrane helix. *J. Biol. Chem. 281*, 15546–15553.
8. Scholze, P., Freissmuth, M., and Sitte, H. H. (2002) Mutations within an intramembrane leucine heptad repeat disrupt oligomer formation of the rat GABA transporter 1. *J. Biol. Chem. 277*, 43682–43690.
9. Thevenin, D., Lazarova, T., Roberts, M. F., and Robinson, C. R. (2005) Oligomerization of the fifth transmembrane domain from the adenosine A2A receptor. *Protein Sci. 14*, 2177–2186.
10. Weimbs, T., and Stoffel, W. (1992) Proteolipid protein (PLP) of CNS myelin: Positions of free, disulfide-bonded, and fatty acid thioester-linked cysteine residues and implications for the membrane topology of PLP. *Biochemistry 31*, 12289–12296.
11. Diaz, R. S., Monreal, J., and Lucas, M. (1990) Calcium movements mediated by proteolipid protein and nucleotides in liposomes prepared with the endogenous lipids from brain white matter. *J. Neurochem. 55*, 1304–1309.
12. Gudz, T. I., Schneider, T. E., Haas, T. A., and Macklin, W. B. (2002) Myelin proteolipid protein forms a complex with integrins and may participate in integrin receptor signaling in oligodendrocytes. *J. Neurosci. 22*, 7398–7407.
13. Kitagawa, K., Sinoway, M. P., Yang, C., Gould, R. M., and Colman, D. R. (1993) A proteolipid protein gene family: Expression in sharks and rays and possible evolution from an ancestral gene encoding a pore-forming polypeptide. *Neuron 11*, 433–448.
14. Swanton, E., Holland, A., High, S., and Woodman, P. (2005) Disease-associated mutations cause premature oligomerization of myelin proteolipid protein in the endoplasmic reticulum. *Proc. Natl. Acad. Sci. U.S.A. 102*, 4342–4347.
15. Brophy, P. J., Horvath, L. I., and Marsh, D. (1984) Stoichiometry and specificity of lipid-protein interaction with myelin proteolipid protein studied by spin-label electron spin resonance. *Biochemistry 23*, 860–865.
16. McLaughlin, M., Hunter, D. J., Thomson, C. E., Yool, D., Kirkham, D., Freer, A. A., and Griffiths, I. R. (2002) Evidence for possible interactions between PLP and DM20 within the myelin sheath. *Glia 39*, 31–36.
17. Sinoway, M. P., Kitagawa, K., Timsit, S., Hashim, G. A., and Colman, D. R. (1994) Proteolipid protein interactions in transfectants: Implications for myelin assembly. *J. Neurosci. Res. 37*, 551–562.
18. Smith, R., Cook, J., and Dickens, P. A. (1984) Structure of the proteolipid protein extracted from bovine central nervous system myelin with nondenaturing detergents. *J. Neurochem. 42*, 306–313.
19. Popot, J. L., Pham Dinh, D., and Dautigny, A. (1991) Major myelin proteolipid: The 4-α-helix topology. *J. Membr. Biol. 123*, 278.
20. Ng, D. P., and Deber, C. M. (2010) Deletion of a terminal residue disrupts oligomerization of a transmembrane α-helix. *Biochem. Cell Biol. 88*, 339–345.
21. Melnyk, R. A., Partridge, A. W., Yip, J., Wu, Y., Goto, N. K., and Deber, C. M. (2003) Polar residue tagging of transmembrane peptides. *Biopolymers 71*, 675–685.
22. Adair, B. D., and Engelman, D. M. (1994) Glycophorin A helical transmembrane domains dimerize in phospholipid bilayers: A resonance energy transfer study. *Biochemistry 33*, 5539–5544.
23. Russ, W. P., and Engelman, D. M. (1999) TOXCAT: A measure of transmembrane helix association in a biological membrane. *Proc. Natl. Acad. Sci. U.S.A. 96*, 863–868.
24. Go, M. Y., Kim, S., Partridge, A. W., Melnyk, R. A., Rath, A., Deber, C. M., and Mogridge, J. (2006) Self-association of the transmembrane domain of an anthrax toxin receptor. *J. Mol. Biol. 360*, 145–156.
25. Johnson, R. M., Rath, A., Melnyk, R. A., and Deber, C. M. (2006) Lipid solvation effects contribute to the affinity of Gly-xxx-Gly motif-mediated helix-helix interactions. *Biochemistry 45*, 8507–8515.
26. Moore, D. T., Berger, B. W., and DeGrado, W. F. (2008) Protein-protein interactions in the membrane: Sequence, structural, and biological motifs. *Structure 16*, 991–1001.
27. Greer, J. M., and Lees, M. B. (2002) Myelin proteolipid protein: The first 50 years. *Int. J. Biochem. Cell Biol. 34*, 211–215.
28. Cunningham, F., and Deber, C. M. (2007) Optimizing synthesis and expression of transmembrane peptides and proteins. *Methods 41*, 370–380.
29. Krishnakumar, S. S., and London, E. (2007) Effect of sequence hydrophobicity and bilayer width upon the minimum length required for the formation of transmembrane helices in membranes. *J. Mol. Biol. 374*, 671–687.
30. Roboti, P., Swanton, E., and High, S. (2009) Differences in endoplasmic-reticulum quality control determine the cellular response to disease-associated mutants of proteolipid protein. *J. Cell Sci. 122*, 3942–3953.
31. Johnson, R. M., Heslop, C. L., and Deber, C. M. (2004) Hydrophobic helical hairpins: Design and packing interactions in membrane environments. *Biochemistry 43*, 14361–14369.
32. Langosch, D., Brosig, B., Kolmar, H., and Fritz, H. J. (1996) Dimerisation of the glycophorin A transmembrane segment in membranes probed with the ToxR transcription activator. *J. Mol. Biol. 263*, 525–530.
33. Yamamoto, T., Nanba, E., Zhang, H., Sasaki, M., Komaki, H., and Takeshita, K. (1998) Jimpy(msd) mouse mutation and connatal Pelizaeus-Merzbacher disease. *Am. J. Med. Genet. 75*, 439–440.
34. Skalidis, G., Trifilieff, E., and Luu, B. (1986) Selective extraction of the DM-20 brain proteolipid. *J. Neurochem. 46*, 297–299.
35. Stenson, P. D., Mort, M., Ball, E. V., Howells, K., Phillips, A. D., Thomas, N. S., and Cooper, D. N. (2009) The Human Gene Mutation Database: 2008 update. *Genome Med. 1*, 13.
36. Lemmon, M. A., Flanagan, J. M., Treutlein, H. R., Zhang, J., and Engelman, D. M. (1992) Sequence specificity in the dimerization of transmembrane α-helices. *Biochemistry 31*, 12719–12725.
37. Smith, N. G., Webster, M. T., and Ellegren, H. (2003) A low rate of simultaneous double-nucleotide mutations in primates. *Mol. Biol. Evol. 20*, 47–53.